CERN-PH-TH/2006-111,
IFJPAN-IV-2006-5

Scalar QED, NLO and PHOTOS Monte Carlo.

G. Nanava
Institute of Nuclear Physics, PAN, Kraków, ul. Radzikowskiego 152, Poland
(On leave from IHEP, TSU, Tbilisi, Georgia)
and
Z. Wąs
CERN, 1211 Geneva 23, Switzerland
and
Institute of Nuclear Physics, PAN, Kraków, ul. Radzikowskiego 152, Poland

ABSTRACT

Recently, due to improvement at experiments, QED bremsstrahlung in B meson decays into pair of scalars (π's and/or K's) is of phenomenological interest. In practical application where experimental acceptance must be taken into account, PHOTOS Monte Carlo is often used for simulation of these QED effects. Phenomenologically sound predictions, valid over all phase space can not be obtained for complex objects, with the scalar QED alone. We will nonetheless use scalar QED to test the performance of PHOTOS. We present the analytical form of the kernel used in the older versions of PHOTOS, and the exact one with respect to first order scalar QED. Matrix element and phase space jacobians are factorized in the final weight. Scalar QED NLO correction weight does not signiticantly improve the predictions. Nonetheless it is necessary for future extensions, such as electromagnetic form-factors.

In this paper we also present aspects of program design, that are related to phase space generation, especially when mass terms become significant; i.e.close to the phase space limits. The discussed effects are way beyond the direct phenomenological interest of today. We use this opportunity to present some foundations of the program organization that assure its precision, which may be useful for future extensions.

Thanks to the applied iteration solution, all leading and next to leading log terms are properly reproduced by the Monte Carlo simulation, and at the higher orders as well. At the same time, full differential distributions over complete multiple body phase space is provided.

An agreement of better than 0.01% with independent calculations of scalar QED is demonstrated. (Distributions varying in densities by up to 8 orders of magnitude are used)

CERN-PH-TH/2006-111,
IFJPAN-IV-2006-5
July, 2006

Supported in part by the EU grant MTKD-CT-2004-510126, in partnership with the CERN Physics Department, and the Polish State Committee for Scientific Research (KBN) grant 2 P03B 091 27 for years 2004-2006.

1. INTRODUCTION

In the analysis of data from high-energy physics experiments, one tries to resolve the "*experiment* = *theory*" equation. This non-trivial task requires that a lot of different effects be considered simultaneously. From the experimental side, these are mainly detector acceptance and cuts, which are dictated by the construction and physical properties of the detector. The shapes of distributions may be distorted by, say, misidentification and residual background contamination. These effects need to be discriminated in an appropriate and well-controlled way. From the theoretical side, *all* effects of known physics have to be included in predictions as well. Only then can experimental data and theoretical predictions be confronted to determine numerical values of coupling constants or effects of new physics (to be discovered).

A well-defined class of theoretical effects consists of QED radiative corrections. PHOTOS is a universal Monte Carlo algorithm that simulates the effects of QED radiative corrections in decays of particles and resonances. It is a project with a rather long history: the first version was released in 1991 [1], followed by version 2.0 [2] (double emission and threshold terms for fermions). The package is in wide use [3]; it was applied as a precision simulation tool for the W mass measurement at the Tevatron [4] and LEP [5, 6], and for CKM matrix measurements in decays of K and B resonances (NA48 [7], KTeV [8] , Belle [9], BaBar [10] and Fermilab [11]). Discussion of the different components of systematic errors in PHOTOS is thus of interest.

Throughout the years the core algorithm for the generation of $O(\alpha)$ corrections did not change much, however, its precision, applicability to various processes, and numerical stability improved significantly. New functionalities, such as multiple photon radiation and interference effects for all possible decays were introduced [12, 13]. Recently, the complete first order matrix element was introduced into PHOTOS for Z decays and complete NLO multiple photon predictions for that channel were demonstrated to work well [14].

Increasing interest in the algorithm expressed by experimental collaborations (including future LHC experiments and precise measurements for B decays) was a motivation to perform a more detailed study of the potential and precision of the PHOTOS algorithm. This paper is devoted to the decay of B mesons into a pair of scalars. It is a continuation of the previous paper [14] devoted to Z decays. Simplifications introduced in the matrix element normally used in these channels are confronted with the exact kernel of first order scalar QED calculation. We concentrate our attention on exact phase-space parametrization as used in PHOTOS, and on the explicit separation of the final weight into parts responsible for: (i) *mass dependent* phase-space Jacobians, (ii) matrix elements and (iii) pre-sampler peaks. Such separation opens the way to include form-factors into matrix elements used in PHOTOS, which can be measured but go beyond scalar QED.

Our study of the PHOTOS algorithm can be understood as another step in the on-going effort to find practical solutions of the improved expansions. The solution can be understood as a rearrangement of the QED perturbation expansion, but this time for the interaction of charged scalars with photons and in case where ultrarelativistic approximations are not valid.

To test PHOTOS we have used predictions of the SANC [15] Monte Carlo algorithm. SANC is able to calculate the exact first order scalar QED matrix elements for decays of B mesons

into scalars, and covers the full phase space of decay products without any approximations. Events provided by SANC MC are unweighted. SANC is a network client-server system for the semi-automatic calculation of Electroweak, QCD and QED radiative corrections at a one-loop precision level for various processes(-decays) of elementary particle interactions.

The paper is organized as follows. Section 2 is devoted to the description of our results obtained from scalar QED, which will be used later in tests. In Section 3 the main properties used in the design of PHOTOS are presented. In particular, the mathematical form of the weight (NLO weight) necessary to introduce the complete first order matrix element. The phase space parametrization necessary to define the iterative solution used in PHOTOS is also given. Section 4 is devoted to results of numerical tests performed at fixed, first order of QED. Numerical tests performed with the multiple bremsstrahlung option will be discussed as well. Finally, section 5 summarizes the paper.

2. Scalar QED and B decays

The one-loop QED correction to the width of the decay $B^{0,-} \to H_1^- H_2^{+,0}$, where $H_{1,2}$ denotes scalar(pseudo-scalar) particles, can be represented as a sum of the Born contribution and the contributions due to virtual loop diagrams and soft and hard photon emissions. Both virtual and soft contributions factorize to the Born one.

$$d\Gamma^{\text{Total}} = d\Gamma^{\text{Born}} \left[1 + \frac{\alpha}{\pi}\left(\delta^{\text{soft}} + \delta^{\text{virt}}\right)\right] + d\Gamma^{\text{Hard}} \tag{1}$$

Here $d\Gamma^{\text{Born}}$ is the tree level differencial decay width, δ^{virt} represents the virtual corrections, δ^{soft} denotes the soft photon contribution and $d\Gamma^{\text{Hard}}$ is the hard photon contribution. The Born level distribution in the rest frame of the decaying meson can be written as

$$d\Gamma^{\text{Born}} = \frac{1}{2M} |A^{\text{Born}}|^2 \, dLips_2(P \to k_1, k_2)\,, \tag{2}$$

where M is the mass of decaying particle, $k_{1,2}$ denote the momenta of decay products, A^{Born} stands for the corresponding tree level amplitude and $dLips_2(P \to k_1, k_2)$ is the two body differential phase space. For the latter we choose the following parametrization

$$dLips_2(P \to k_1, k_2) = \frac{1}{32\pi^2} \frac{\lambda^{1/2}(M^2, m_1^2, m_2^2)}{M^2} d\cos\theta_1 d\phi_1, \tag{3}$$

where angles θ_1 and ϕ_1 define the orientation of momentum k_1 in the rest frame of B. In the case of neutral B meson decay channels $B^0 \to H_1^- H_2^+$, the scalar QED calculation for the virtual

and soft factors in formula (1) gives

$$\begin{aligned}
\delta^{\rm virt} &= \left[1+\frac{M^2-m_1^2-m_2^2}{\Lambda}\ln\frac{2m_1m_2}{M^2-m_1^2-m_2^2+\Lambda}\right]\ln\frac{M^2}{m_\gamma^2}+\frac{3}{2}\ln\frac{\mu_{UV}^2}{M^2}\\
&+ \frac{M^2-m_1^2-m_2^2}{2\Lambda}\left[{\rm Li}_2\left(\frac{M^2+m_1^2-m_2^2+\Lambda}{2\Lambda}\right)-{\rm Li}_2\left(\frac{-M^2+m_2^2-m_1^2+\Lambda}{2\Lambda}\right)\right.\\
&\qquad\left.+2\ln\frac{2Mm_1}{M^2+m_1^2-m_2^2+\Lambda}\ln\frac{m_1\Lambda}{M^3}+(1\leftrightarrow 2)+\pi^2\right]\\
&- \frac{\Lambda}{2M^2}\ln\frac{2m_1m_2}{M^2-m_1^2-m_2^2+\Lambda}+\frac{m_2^2-m_1^2}{4M^2}\ln\frac{m_2^2}{m_1^2}-\frac{1}{2}\ln\frac{m_1m_2}{M^2}+1; \qquad (4)
\end{aligned}$$

$$\begin{aligned}
\delta^{\rm soft} &= \left[1+\frac{M^2-m_1^2-m_2^2}{\Lambda}\ln\frac{2m_1m_2}{M^2-m_1^2-m_2^2+\Lambda}\right]\ln\frac{m_\gamma^2}{4\omega^2}\\
&+ \frac{M^2-m_1^2-m_2^2}{2\Lambda}\left[{\rm Li}_2\left(\frac{-2\Lambda}{M^2+m_1^2-m_2^2-\Lambda}\right)-{\rm Li}_2\left(\frac{2\Lambda}{M^2+m_1^2-m_2^2+\Lambda}\right)+(1\leftrightarrow 2)\right]\\
&- \frac{M^2+m_1^2-m_2^2}{\Lambda}\ln\frac{2Mm_1}{M^2+m_1^2-m_2^2+\Lambda}-(1\leftrightarrow 2), \qquad (5)
\end{aligned}$$

where, $m_{1,2}$ are the final meson masses, ω is the soft-hard photon separator, and μ_{UV} denotes the ultraviolet scale. The infrared divergence is regularized by the photon mass m_γ.
$\Lambda=\lambda^{1/2}(M^2,m_1^2,m_2^2)$ and ${\rm Li}_2(z)=-\int_0^z\frac{dy}{y}\ln(1-y)$.
The hard photon distribution $d\Gamma^{\rm Hard}$ in scalar QED can be expressed as follows

$$d\Gamma^{\rm Hard}=\frac{1}{2M}|A^{\rm Born}|^2 4\pi\alpha\left(q_1\frac{k_1.\varepsilon}{k_1.k_\gamma}-q_2\frac{k_2.\varepsilon}{k_2.k_\gamma}\right)^2 dLips_3(P\to k_1,k_2,k_\gamma), \qquad (6)$$

here, $q_{1,2}$ are the charges of final mesons, and k_γ and ε_μ are the photon momentum and polarization vector respectively. The three body differential phase space of the decay products $dLips_3(P\to k_1,k_2,k_\gamma)$, is parametrized as follows:

$$dLips_3(P\to k_1,k_2,k_\gamma)=\frac{\lambda^{1/2}(1-2E_\gamma/M,m_1^2/M^2,m_2^2/M^2)}{16(2\pi)^5\,(1-2E_\gamma/M)}E_\gamma dE_\gamma d\cos\theta_\gamma d\phi_\gamma d\cos\theta_1^R d\phi_1^R, \qquad (7)$$

where the angles θ_1^R, ϕ_1^R define the orientation of momentum k_1 in the rest frame of (k_1+k_2); and the photon energy E_γ, and the angles θ_γ and ϕ_γ that define the photon momentum, are given in the rest frame of the decaying particle. These parameters vary in the limits: $0\le\theta_\gamma,\theta_1^R\le\pi$, $0\le\phi_\gamma,\phi_1^R\le 2\pi$ and $\omega\le E_\gamma\le(M^2-(m_1+m_2)^2)/2M$. After integration of (6) over the phase space variables (7), in the massless limit of the final mesons (i.e. $m_{1},m_{2}\equiv m\to 0$), we obtain

$$\Gamma^{\rm Hard}=\Gamma^{\rm Born}\frac{\alpha}{\pi}\left[\left(1-\ln\frac{m^2}{M^2}\right)\ln\frac{4\omega^2}{M^2}-2\ln\frac{m^2}{M^2}-\frac{\pi^2}{3}+4\right]. \qquad (8)$$

The virtual correction depends on the ultraviolet scale μ_{UV}, which should cancel in the total decay width because of the scale dependence of the point-like weak coupling. The infrared divergence cancels in the sum of virtual and soft contributions, as it must. The total width, which is sum of the contributions (4), (5), and (8), is also free of ω and of the final meson mass singularity in accordance with the KLN theorem [16]– [17]:

$$\Gamma^{\rm Total} = \Gamma^{\rm Born}\left[1+\frac{\alpha}{\pi}\left(\frac{3}{2}\ln\frac{\mu_{UV}^2}{M^2}+5\right)\right]. \tag{9}$$

The same calculations can be done for the charged B meson decay channels $B^- \to H_1^- H_2^0$.
– Virtual photon contribution,

$$\begin{aligned}
\delta^{\rm virt} &= \left[1+\frac{M^2+m_1^2-m_2^2}{\Lambda}\ln\frac{2Mm_1}{M^2+m_1^2-m_2^2+\Lambda}\right]\ln\frac{Mm_1}{m_\gamma^2}+\frac{3}{2}\ln\frac{\mu_{UV}^2}{Mm_1} \\
&+ \frac{M^2+m_1^2-m_2^2}{2\Lambda}\left[{\rm Li}_2\left(\frac{M^2-m_1^2-m_2^2+\Lambda}{2\Lambda}\right)-{\rm Li}_2\left(\frac{M^2-m_1^2-m_2^2-\Lambda}{-2\Lambda}\right)\right. \\
&\qquad + {\rm Li}_2\left(\frac{M^2+m_2^2-m_1^2-\Lambda}{-2\Lambda}\right)-{\rm Li}_2\left(\frac{M^2+m_2^2-m_1^2+\Lambda}{2\Lambda}\right) \\
&\qquad \left. + 2\ln\frac{2Mm_1}{M^2+m_1^2-m_2^2+\Lambda}\ln\frac{\Lambda}{Mm_2}-\ln\frac{2Mm_2}{M^2+m_2^2-m_1^2+\Lambda}\ln\frac{M^2}{m_1^2}\right] \\
&+ \frac{\Lambda}{2m_2^2}\ln\frac{2Mm_1}{M^2+m_1^2-m_2^2+\Lambda}-\frac{M^2-m_1^2}{4m_2^2}\ln\frac{m_1^2}{M^2}+1;
\end{aligned} \tag{10}$$

– Soft photon contribution,

$$\begin{aligned}
\delta^{\rm soft} &= \left[1+\frac{M^2+m_1^2-m_2^2}{\Lambda}\ln\frac{2Mm_1}{M^2+m_1^2-m_2^2+\Lambda}\right]\ln\frac{m_\gamma^2}{4\omega^2} \\
&+ \frac{M^2+m_1^2-m_2^2}{2\Lambda}\left[{\rm Li}_2\left(\frac{-2\Lambda}{M^2+m_1^2-m_2^2-\Lambda}\right)-{\rm Li}_2\left(\frac{2\Lambda}{M^2+m_1^2-m_2^2+\Lambda}\right)\right] \\
&- \frac{M^2+m_1^2-m_2^2}{2\Lambda}\ln\frac{2Mm_1}{M^2+m_1^2-m_2^2+\Lambda};
\end{aligned} \tag{11}$$

– Hard photon contribution,

$$\begin{aligned}
d\Gamma^{\rm Hard} &= \frac{1}{2M}|A^{\rm Born}|^2 4\pi\alpha\left(q_1\frac{k_1.\varepsilon}{k_1.k_\gamma}-q\frac{P.\varepsilon}{P.k_\gamma}\right)^2 dLips_3(P\to k_1,k_2,k_\gamma), \\
\Gamma^{\rm Hard} &= \Gamma^{\rm Born}\frac{\alpha}{\pi}\left[\left(1+\frac{1}{2}\ln\frac{m^2}{M^2}\right)\ln\frac{4\omega^2}{M^2}+\ln\frac{m^2}{M^2}-\frac{\pi^2}{6}+3\right].
\end{aligned} \tag{12}$$

Again after integration over the phase space, the massless limit of the final mesons (i.e. $m_1, m_2 \equiv m \to 0$) was used in this formula. Finally, summing contributions (12), (11) and (10), we obtain

the following for the total decay width:

$$\Gamma^{\rm Total} \;=\; \Gamma^{\rm Born}\left[1+\frac{\alpha}{\pi}\left(\frac{3}{2}\ln\frac{\mu_{UV}^2}{M^2}-\frac{\pi^2}{3}+\frac{11}{2}\right)\right]. \tag{13}$$

We have checked that the factors $\delta^{\rm soft}$ and $\delta^{\rm virt}$ provide the same numerical results (at double precision level) as the corresponding expressions from [18].

To be assured of the accuracy of SANC Monte Carlo integration (which is a by-product of MC simulation), we compared Monte Carlo results with the analytical calculations. For instance, the analytical result for total width of the decay $B^0\to K^+K^-(\gamma)$ was $\Gamma^{\rm Total}_{\rm AC}=0.000370096$ MeV, while SANC Monte Carlo gave $\Gamma^{\rm Total}_{\rm MC}=0.0003700(6)$ MeV. For the channel $B^-\to K^-K^0(\gamma)$ we got respectively $\Gamma^{\rm Total}_{\rm AC}=0.000377615$ MeV, $\Gamma^{\rm Total}_{\rm MC}=0.0003776(2)$ MeV[1]. The agreement is thus better than 10^{-4} in this test, where mass effects were included.

3. Exact phase-space and matrix element.

To start any discussion of the implementation of complete first order QED radiative corrections in B decay, one has to specify the parametrization of the complete phase-space slots of the fixed final state multiplicity.

Let us start with the explicit expression for the parametrization of an $n+1$ body phase-space in decay of the object of four-momentum P, as used in PHOTOS Monte Carlo. As our aim is to define iterative relations, let us denote the four momenta of the first n decay products as k_i and the last $n+1$ decay product as q. In our case the $n+1$-th particle will always be the real and massless photon[2]. In the later steps of our construction the masslessnes of photons and properties of QED matrix elements will be used.

In the following, notation from Refs. [19,20] will be used. We will not rely on any particular results of these papers. We only point to other, similar options for the exact n-body phase-space parameterizations, which are used for other purposes.

The Lorentz invariant phase-space is defined as follows:

$$\begin{aligned}
&dLips_{n+1}(P) = \\
&\frac{d^3k_1}{2k_1^0(2\pi)^3}\cdots\frac{d^3k_n}{2k_n^0(2\pi)^3}\frac{d^3q}{2q^0(2\pi)^3}(2\pi)^4\delta^4\Big(P-\sum_1^n k_i-q\Big) \\
=\;& d^4p\,\delta^4(P-p-q)\frac{d^3q}{2q^0(2\pi)^3}\frac{d^3k_1}{2k_1^0(2\pi)^3}\cdots\frac{d^3k_n}{2k_n^0(2\pi)^3}(2\pi)^4\delta^4\Big(p-\sum_1^n k_i\Big) \\
=\;& d^4p\,\delta^4(P-p-q)\frac{d^3q}{2q^0(2\pi)^3}dLips_n(p\to k_1\ldots k_n),
\end{aligned} \tag{14}$$

[1] Please note that these numbers are for the purpose of our test only, the overall $B-H-H$ coupling constants do not match the experimental data

[2] However the construction does not rely on a photon to be masless. In principle it can be applied to define other phase space relations, for example the emission of an extra massive pion or emission of a pair of heavy particles.

where extra integration variables, four vector p (compensated with $\delta^4\left(p-\sum_1^n k_i\right)$) and M_1 (compensated with $\delta\left(p^2-M_1^2\right)$) are introduced. The element of the phase space integration takes the form:

$$\begin{aligned} & dLips_{n+1}(P) = \\ & \frac{dM_1^2}{(2\pi)} dLips_2(P \to p\ q) \times dLips_n(p \to k_1 \ldots k_n) \\ = \quad & dM_1^2 \left[d\cos\theta d\phi \frac{1}{8(2\pi)^3} \frac{\lambda^{\frac{1}{2}}(M^2, M_1^2, q^2)}{M^2} \right] \times dLips_n(p \to k_1 \ldots k_n). \end{aligned} \tag{15}$$

The part of the phase space jacobian corresponding to integration over the direction and energy of the last particle (or equvalently invariant mass M_1 of the remaining system) is explicitly given. As usual we define $\lambda^{\frac{1}{2}}(a,b,c) = \sqrt{a^2+b^2+c^2-2ab-2ac-2bc}$. The integration over the angles θ and ϕ is defined in the rest frame of the $n+1$ particles. The integration over the invariant mass, M_1, is limited by phase space boundaries. The question of choice of axes with respect to which angles are defined is not trivial. Many options exist, we will not elaborate on that point here. It is covered in Ref. [1]. Formula (15) can be iterated and provide a parametrization of the phase space with an arbitrary number of final state particles. In such a case, the question of orientation of the frames used to define the angles and the order of M_i integrations (consequently, the choice of limits for M_i integration), becomes particularly rich. Our choice is defined in Ref. [2]. We will not elaborate on this interesting point here, nothing new was necessary for the purpose of our study. Except for the mentioned above details, the choice used for our phase space organization is the same as in FOWL [21], TAUOLA [20] and probably many other generators as well.

If the invariant mass of the system of all particles except the first one M_1, is replaced with the energy of the first one defined in the P rest-frame, k_γ, and the simplification due to zero photon mass is used, then the phase space formula can be written as:

$$\begin{aligned} & dLips_{n+1}(P) = \\ & \left[4dk_\gamma k_\gamma d\cos\theta d\phi \frac{1}{8(2\pi)^3} \right] \times dLips_n(p \to k_1 \ldots k_n) \\ = \quad & \left[k_\gamma dk_\gamma d\cos\theta d\phi \frac{1}{2(2\pi)^3} \right] \times dLips_n(p \to k_1 \ldots k_n), \end{aligned} \tag{16}$$

If we would have l photons accompanying n other particles, then the factor in square brackets is iterated. The statistical factor $\frac{1}{l!}$ would complete the form of the phase space parametrization, similar to the formal expansion of the exponent. The last formula, supplemented with definition of frames with respect to which angles are defined is used to define the full kinematic configuration of the event. From angles and energies (k_{γ_i}) of photons and also angles and masses for other decay products, four-momenta of all final state particles can be constructed.

If in formula (16) instead of $dLips_n(p \to k_1 \ldots k_n)$ one would use $dLips_n(P \to k_1 \ldots k_n)$ the **tangent space** would be obtained. Then photons do not affect other particles' momenta at all, and have no boundaries on energies or directions. Photons are independent from one another as

well[3]. The tangent space is unbounded from above. Energy and momentum conservation define relation between tangent and real phase space. The formula defining one step in the iteration reads as follows:

$$\begin{aligned} &dLips_{n+1}(P) = \\ &\left[4dk_\gamma k_\gamma d\cos\theta d\phi \frac{1}{8(2\pi)^3} \times \frac{\lambda^{1/2}(1, m_1^2/p^2, M_2^2/p^2)}{\lambda^{1/2}(1, m_1^2/P^2, M_2^2/P^2)}\right] \\ &\times dLips_n(P \to \bar{k}_1 ... \bar{k}_n), \end{aligned} \tag{17}$$

and can be obtained from formula (15). We have to use this formula for $Lips_{n+1}(P \to k_\gamma k_1 ... k_n)$ twice:

$$\begin{aligned} Lips_{n+1}(P \to k_\gamma k_1 ... k_n) &= \frac{dM_1^2}{(2\pi)} Lips_2(P \to k_\gamma p) \times Lips_n(p \to k_1 ... k_n) \\ Lips_n(p \to k_1 ... k_n) &= \frac{dM_2^2}{(2\pi)} Lips_2(p \to k_1 p') \times Lips_{n-1}(p' \to k_2 ... k_n) \end{aligned} \tag{18}$$

and compare it with:

$$Lips_n(P \to \bar{k}_1 ... \bar{k}_n) = \frac{dM_2^2}{(2\pi)} Lips_2(P \to \bar{k}_1 \bar{p}') \times Lips_{n-1}(\bar{p}' \to \bar{k}_2 ... \bar{k}_n). \tag{19}$$

where the factors $Lips_2(p \to k_1 p') \times Lips_{n-1}(p' \to k_2 ... k_n)$ and $Lips_{n-1}(\bar{p}' \to \bar{k}_2 ... \bar{k}_n)$ are chosen to match and relate with a common boost L: $\bar{p}' = Lp'$, $\bar{k}_2 = Lk_2$,..., $\bar{k}_n = Lk_n$, finally $p'^2 = M_2^2$. We skip details of the particular orientation of the frames. We direct the reader to Refs. [1, 2] for that purpose. Let us remark that formula (17) is an example: many options can be introduced, necessary, for example in the case when PHOTOS is used for the intermediate decay of large chain of subsequent decays.

Formula (17) can be realized algorithmically in the following way:

1. For any point in n-body phase space (earlier generated event), described for example with the explicit configuration of four vectors $\bar{k}_1 ... \bar{k}_n$, coordinate variables can be calculated, using formula (15).

2. Photon variables can be generated according to the expression in square brackets of Eq. (16).

3. Obtained in this way variables from the old configuration and the one of a photon can be used to construct the new kinematical configuration for the $n+1$-body final state. The phase-space weight, which is zero for configurations outside phase space boundaries, can be calculated at this point from (17) and finally combined with the matrix element.

[3]Expression (16) would be only slightly more complicated if instead of photons a massive particle was to be added.

The presentation of the above example is incomplete and in practice a lot of options need to be used. Here we have chosen two sub-groups of n-body phase space. The first one consisted from particle 1 and the second from particles 2 to n combined together. Obviously in case of 2-body decays discussed in this paper, choices are limited.

We can generalize formula (17) to the case of l photons by iteration, in exactly the same manner as was done for formula (16). If the expresion in brackets in Eq. (17) is dropped we may define:

$$\begin{aligned} & dLips_{n+l}(P) = \\ = \; & \frac{1}{l!}\prod_{i=1}^{l}\left[k_{\gamma_i}dk_\gamma d\cos\theta_i d\phi_i \frac{1}{2(2\pi)^3}\right] \times dLips_n(P \to k_1 ... k_n), \end{aligned} \tag{20}$$

as the **tangent space** for the multiple photon configuration. Photons do not affect other particles' momenta. They also have no boundaries on energy and are independent one from another. It is important to realize that one has to choose matrix elements for the tangent space to define the transformation to the real space. Rejection and event construction, performed with the help of formula (17) for each consecutive photon, diminish photon multiplicity. At the same time, energy-momentum conservation constraints are introduced. Of course as rejection implements changes in phase space density, a matrix element, that includes virtual corrections, should be taken as well. This is equally true for the tangent-space and the physical space.

The treatment of the phase space presented here lies at the heart of the construction of PHOTOS kinematics, and was used since its beginning. It exhausts the case when there is only one charged particle in final state. Case of multiple charged particles final states, when some of them are ultrarelativistic, collinear configuartion need attention; presampler with multichannel generation is needed. In our case we follow the same method[4] as explained in Ref. [20]. For generation, the exact phase-space parametrization is not sufficient. It must be completed with the matrix element, with both virtual and real bremsstrahlung QED corrections taken into account. Careful regularization of soft singularities has to be performed as well.

In the standard version of PHOTOS, as published in [1, 2], the following matrix element is used for single photon emission when there is only one charged particle in final state:

$$|\mathcal{M}|^2_{PHOTOS} \;=\; |A^{\rm Born}|^2 WT_3 \tag{21}$$

where

$$\begin{aligned} WT_3^{old} &= \frac{4\pi\alpha}{WT_1 WT_2}\frac{2(1-x)}{1+(1-x)^2}\left(1-\frac{m_R^2}{1-\beta^2\cos^2\theta}\right)\frac{1+\beta\cos\theta}{2}\frac{1-\sqrt{1-m_R^2}\cos\theta}{1-\beta\cos\theta} \\ \beta &= \sqrt{1-4\frac{m_1^2}{M^2(1-x)}\frac{1}{(1-x+(m_1^2-m_2^2)/M^2)^2}} \\ x &= \frac{2E_\gamma}{M}\frac{M^2}{M^2-(m_1+m_2)^2}, \quad m_R^2 = 4\frac{m_1^2}{M^2(1+m_1^2/M^2)^2}. \end{aligned}$$

[4] We will omit details here, because for the two-body final states and obviously massless photon, the necessary complications manifest themselves only in the case of multiple photon generation. We will not explain this subject in detail here.

This old and somehow awkward approximation WT_3^{old} for WT_3 implemented in standard PHOTOS is present due to historical reasons. The expression without approximations reads:

$$\begin{aligned}
|\mathcal{M}|^2_{exact} &= |A^{\rm Born}|^2 4\pi\alpha \left(q_1 \frac{k_1.\varepsilon}{k_1.k_\gamma} - q \frac{P.\varepsilon}{P.k_\gamma} \right)^2 \\
&= |A^{\rm Born}|^2 4\pi\alpha \, \frac{8}{M^2} \times \frac{\lambda\left(1, \frac{m_1^2}{\tau}, \frac{m_2^2}{\tau}\right)\left(1 - \frac{2E_\gamma}{M}\right)\sin^2\theta}{2\left(\frac{2E_\gamma}{M}\right)^2 \left(1 + \frac{m_1^2 - m_2^2}{\tau} - \lambda^{1/2}\left(1, \frac{m_1^2}{\tau}, \frac{m_2^2}{\tau}\right)\cos\theta\right)^2} \\
&= |A^{\rm Born}|^2 4\pi\alpha \, \frac{8}{M^2} \times WT_3(P, k_1, k_2, k_\gamma)
\end{aligned} \tag{22}$$

here, $(k_1 + k_2)^2 = \tau$. In both, the standard and exact version of PHOTOS the same phase-space parametrization and presampler for collinear and soft singularities are used, the appropriate contributions to the final weight read:

$$\begin{aligned}
WT_1(P, k_1, k_2, k_\gamma) &= \frac{\lambda^{1/2}\left(1, \frac{m_1^2}{M^2}, \frac{m_2^2}{M^2}\right)}{\lambda^{1/2}\left(1, \frac{m_1^2}{\tau}, \frac{m_2^2}{\tau}\right)} \frac{2E_\gamma}{M} \\
WT_2(P, k_1, k_2, k_\gamma) &= \frac{2(1 - \cos\theta\sqrt{1 - m_R^2})}{1 + (1 - x)^2} \frac{M}{2E_\gamma}
\end{aligned} \tag{23}$$

The expression for WT_1 can be deciphered from formula (17) and WT_2 is related to presamplers for collinear and soft singularities. Together with WT_3 for the matrix element, they are implemented in routine `PHOCOR` of PHOTOS. The following defines the notations used. The photon energy E_γ is defined in rest frame of the decaying particle (of mass M). Masses of decaying particles are denoted respectively as m_1 and m_2. The angle θ between directions of k_1 and k_γ is defined in the rest-frame of $k_1 + k_2$.

The combined effect of the virtual and real corrections on the total rate increases by a factor of $\frac{\Gamma^{\rm Total}}{\Gamma^{\rm Born}}$. The ratio of (22) and (21) constitutes the basic element of upgrading PHOTOS functionality to the complete first order[5]. Nothing had to be changed in the phase space parametrization. Effects of virtual corrections need to be included as well, and must be included in the normalization. The correcting weight can be chosen simply as:

$$wt = \frac{|\mathcal{M}|^2_{exact}}{|\mathcal{M}|^2_{PHOTOS}} \frac{\Gamma^{\rm Born}}{\Gamma^{\rm Total}}. \tag{24}$$

For the standard version of PHOTOS the virtual corrections are required to be such that the total decay rate remains unchanged after complete QED corrections are included.

[5]This is only true in the case when PHOTOS is run at the first order. When option of multiple radiation is used in PHOTOS, the single photon emission kernel is iterated. This lead to some complications.

In case of final states with two charged particles in PHOTOS the following versions of the interference weight were used:

$$\begin{aligned}
WT_{INT} &= \frac{\left(q_1\frac{k_1.\varepsilon}{k_1.k_\gamma}-q_2\frac{k_2.\varepsilon}{k_2.k_\gamma}\right)^2}{\left(q_1\frac{k_1.\varepsilon}{k_1.k_\gamma}-q\frac{P.\varepsilon}{P.k_\gamma}\right)^2+\left(q_1\frac{k_2.\varepsilon}{k_2.k_\gamma}-q\frac{P.\varepsilon}{P.k_\gamma}\right)^2} \\
WT_{INT-option} &= J_{1,2}\frac{\left(q_1\frac{k_1.\varepsilon}{k_1.k_\gamma}-q_2\frac{k_2.\varepsilon}{k_2.k_\gamma}\right)^2}{\left(q_1\frac{k_1.\varepsilon}{k_1.k_\gamma}-q\frac{P.\varepsilon}{P.k_\gamma}\right)^2 J_1+\left(q_1\frac{k_2.\varepsilon}{k_2.k_\gamma}-q\frac{P.\varepsilon}{P.k_\gamma}\right)^2 J_2} \\
J_1 &= \frac{1}{WT_1(P,k_1,k_2,k_\gamma)WT_2(P,k_1,k_2,k_\gamma)} \\
J_2 &= \frac{1}{WT_1(P,k_2,k_1,k_\gamma)WT_2(P,k_2,k_1,k_\gamma)}
\end{aligned} \tag{25}$$

The form of WT_{INT} results from the exact expressions, formulae (12) and (6). However, phase space and multichannel presampler specific terms (23) need to be discussed. Presence of J_1 and J_2 in interference weight is optional, but only for single photon radiation. The factor $J_{1,2}$ (J_1 or J_2) must cancel the $WT_1 \cdot WT_2$ term of the generation branch used for this particular event generation. In general, the absence of J_i terms is due to properties of the second order matrix element[6]. These will not be discussed here. For the time being identified similarities with the case of Z decay have to be used instead.

Once we have completed the description of our internal correcting weight necessary for PHOTOS to work in the NLO regime, we will turn to the numerical results.

[6]For example the form $WT_{INT-option}$ is inappropriate for configurations when the first generated photon is hard and the second soft.

4. Results of the tests

The most attractive property of Monte Carlo is the possibility to implement selection criteria for the theoretical predictions that coincide with the experimental ones. Especially in the case of the final state bremsstrahlung presence of experimental cut-offs is essential, as they usually significantly increase the size of the QED effects.

In this section we will concentrate however, on the following pseudo-observables, as used in Ref. [22, 23]:

- **-A-** *Photon energy in the decaying particle rest frame:* this observable is sensitive mainly to the leading-log (i.e. collinear) non-infrared (i.e. not soft) component of the distributions.

- **-B-** *Energy of the final-state charged particle:* as the previous one, this observable is sensitive mainly to the leading-log (i.e. collinear) non-infrared (i.e. not soft) component of the distributions.

- **-C-** *Angle of the photon with final-state charged particle:* this observable is sensitive mainly to the non-collinear (i.e. non-leading-log) but soft (i.e. infrared) component of the distributions.

- **-D-** *Acollinearity angle of the final-state scalars:* this observable is sensitive mainly to the non-collinear (i.e. non-leading-log) and non-soft (i.e. non-infrared) component of the distributions.

We will start our comparison for $B^- \to \pi^0 K^-(\gamma)$ and PHOTOS running without improvements from the complete matrix element. Despite this fact the agreement looks good, see fig. 1, and holds over the entire range of the distributions, which varies by up to 6 orders of magnitude. Differences can hardly be seen. To visualize the differences, in fig. 2, the ratios of the distributions are plotted. Similar to what was seen in the tests for Z decays [14] local discrepancies may reach up to 15 % for $\cos\theta_{acoll.} > 0.5$. Note however that those regions of the phase-space contribute at the level of 10^{-6} to the total decay rate. Once the matrix element is switched on, see fig. 3, where ratios of distribution are plotted, the agreement become excellent, even at a statistical level of 10^9 events. It was of no use to repeat the plots of the distributions with the corrected weight in PHOTOS, as the plots could not be distinguished from the ones of fig. 1.

Encouraged by the excellent performance in the case of the decay into final states with a single charged particle, let us now turn to decays into two charged mesons. To avoid accidental simplifications, we have selected final states with scalars of different masses ($B^0 \to \pi^- K^+(\gamma)$).

Again, as can be seen from figs. 4 and 5, agreement between PHOTOS using the standard kernel and SANC is rather good, but some differences persist. Once the complete kernel is switched on, fig. 6, the agreement is quite amazing. In this case, the interference weight, and the multiple singularity structure of the pre-sampler Jacobians, formula (25), were tested as well. Both versions WT_{INT} and $WT_{INT-option}$ gave the same results for the case of single

Figure 1: Results from PHOTOS, standard version, and SANC for $B^- \to \pi^0 K^-(\gamma)$ decay are superimposed on the consecutive plots. Standard distributions, as defined in the text, are used. Logarithmic scales are used. The distributions from the two plots overlap almost completely. Samples of 10^9 events were used.

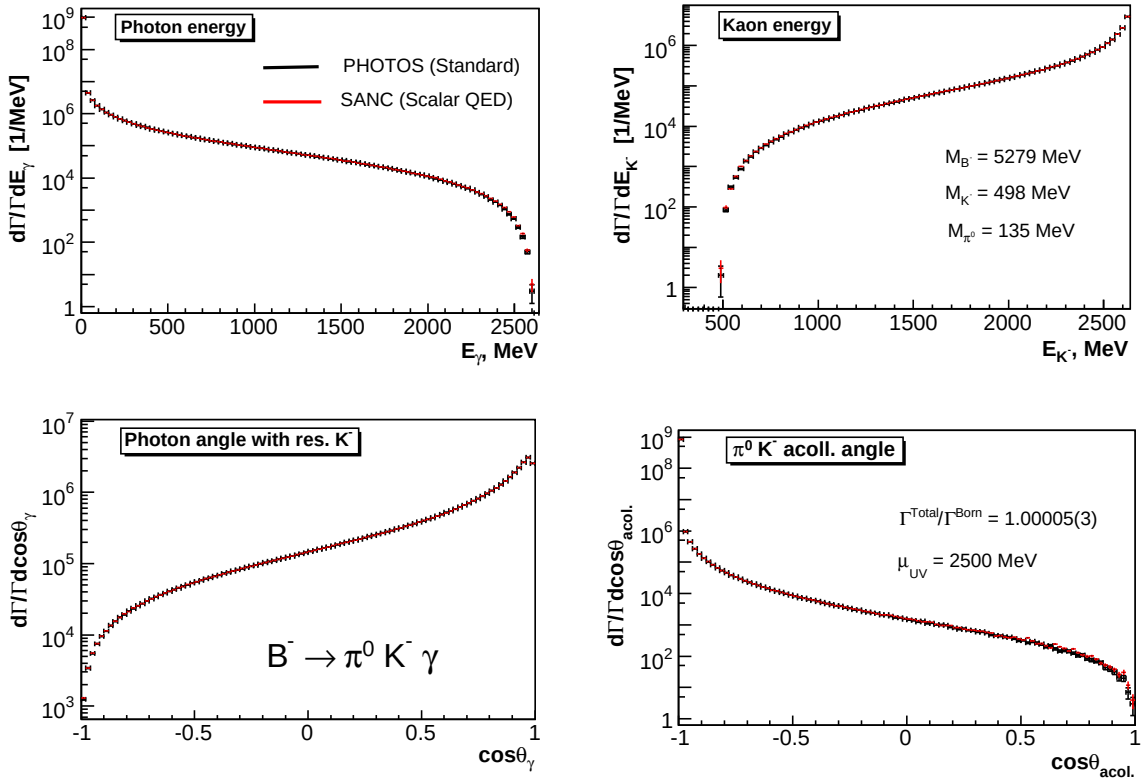

Figure 2: Results from PHOTOS, standard version, and SANC for ratios of the $B^- \to \pi^0 K^-(\gamma)$ distributions in fig.1 are presented. Differences between PHOTOS and SANC are small, but are clearly visible now.

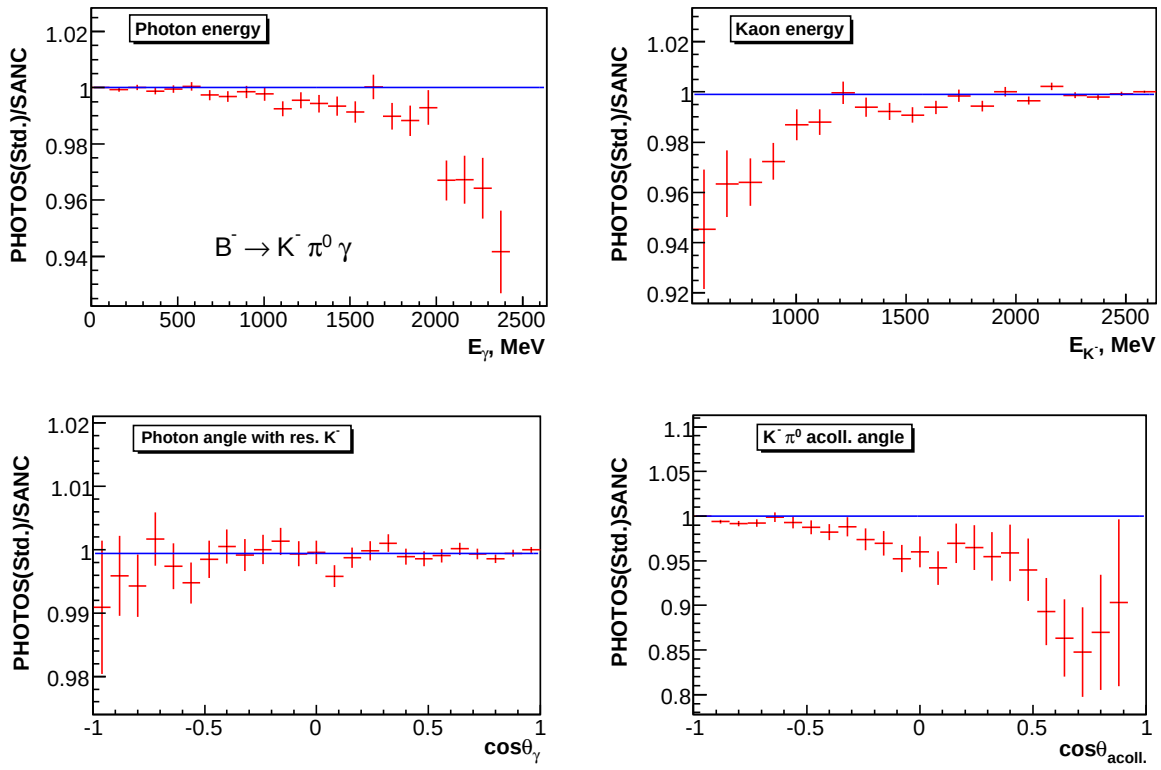

Figure 3: Results from PHOTOS with the exact matrix element, and SANC for ratios of the $B^- \to \pi^0 K^-(\gamma)$ distributions. Differences between PHOTOS and SANC are below statistical error for samples of 10^9 events.

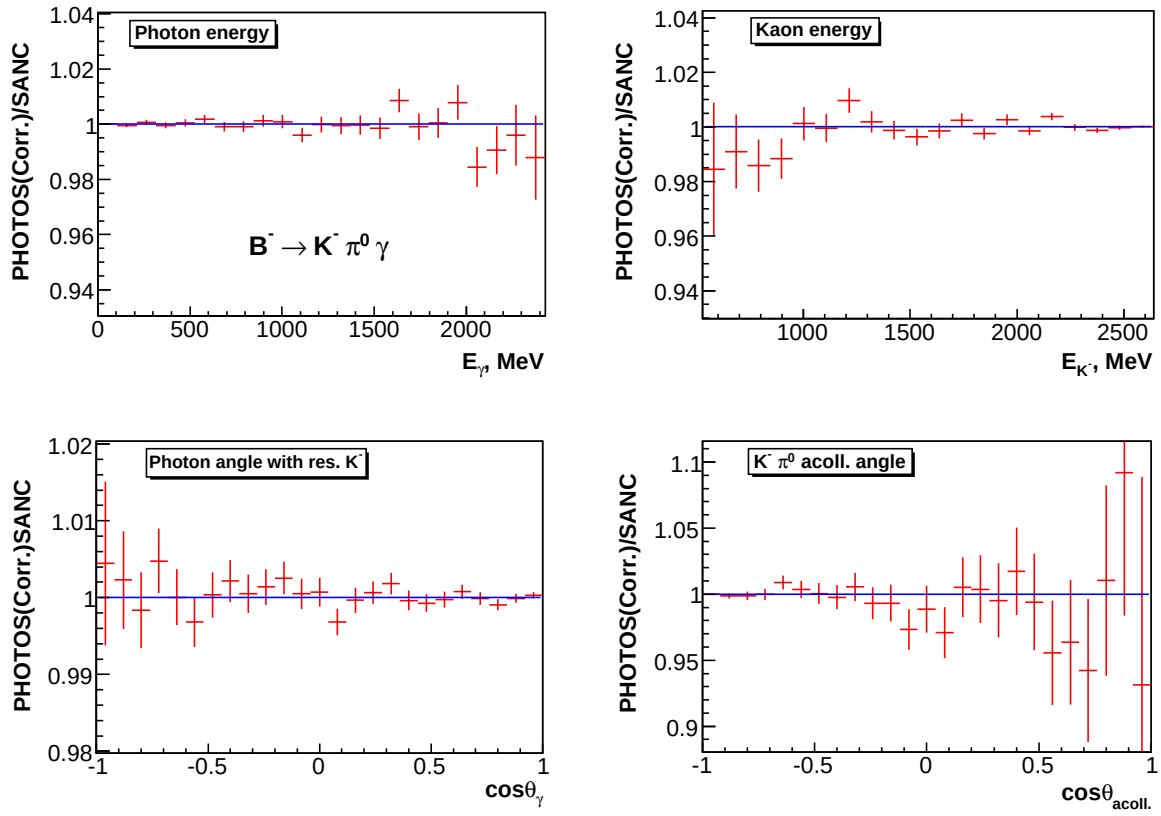

Figure 4: Results from PHOTOS, standard version, and SANC for $B^0 \to \pi^- K^+(\gamma)$ decay are superimposed on the consecutive plots. Standard distributions, as defined in the text, are used. Logarithmic scales are used. The distributions from the two plots overlap almost completely. Samples of 10^9 events were used.

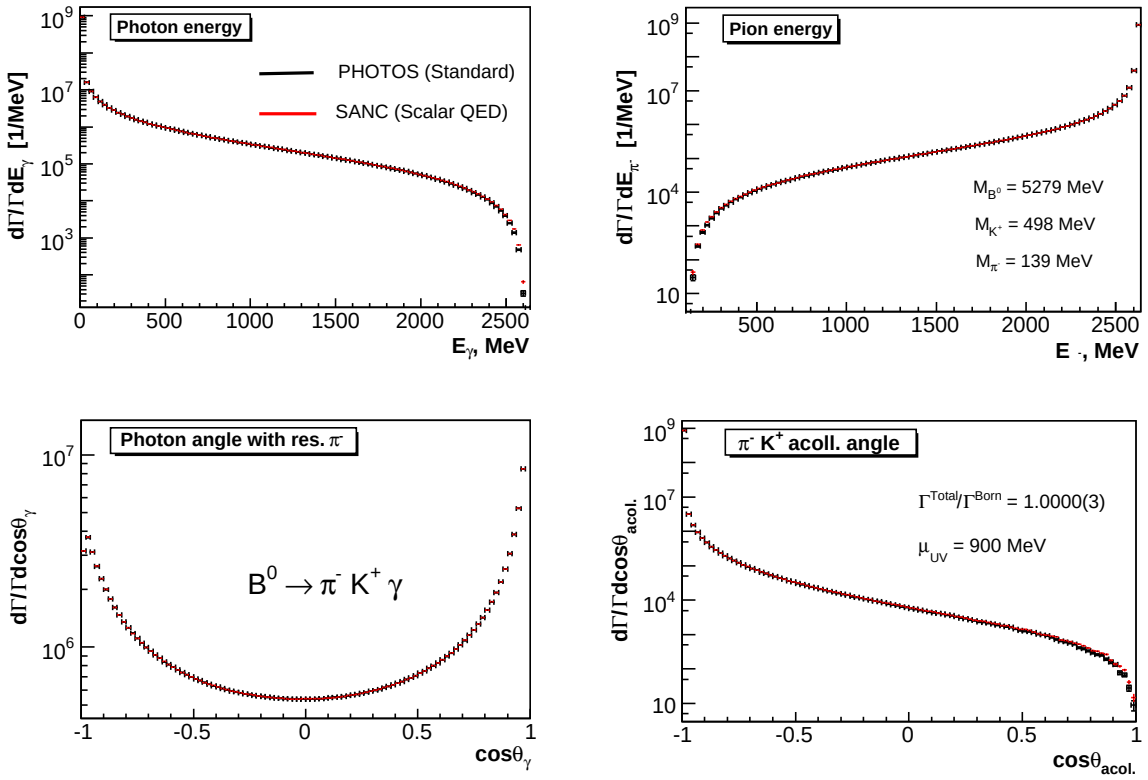

photon emission. However only the first version, WT_{INT} turned out to be consistent with exponentiation. We will skip discussion of this point here. To complete the tests of phase-space for multichannel emissions, final states with more than two massive decay products need to be studied, preferably for multiphoton radiation as well.

Let us comment that not only the shapes of the distribution agree in an excellent manner between PHOTOS and SANC simulations, also the number of events with photons of energy below the certain threshold agreed better than 0.01 %, thus were consistent with each other within a statistical error of 10^9 event samples. The excellent agreement, presented in our paper, combined with other results published before, help to confirm that theoretical effects normally missing in PHOTOS are small, but if necessary can be introduced into the code. It is also important to note that the agreement provides powerful technical test of the generator.

Finally, let us point out that early versions of the program, before 2004, were not reaching

Figure 5: Results from PHOTOS, standard version, and SANC for ratios of the $B^0 \to \pi^- K^+(\gamma)$ distributions in fig.4 are presented. Differences between PHOTOS and SANC are small, but are clearly visible now.

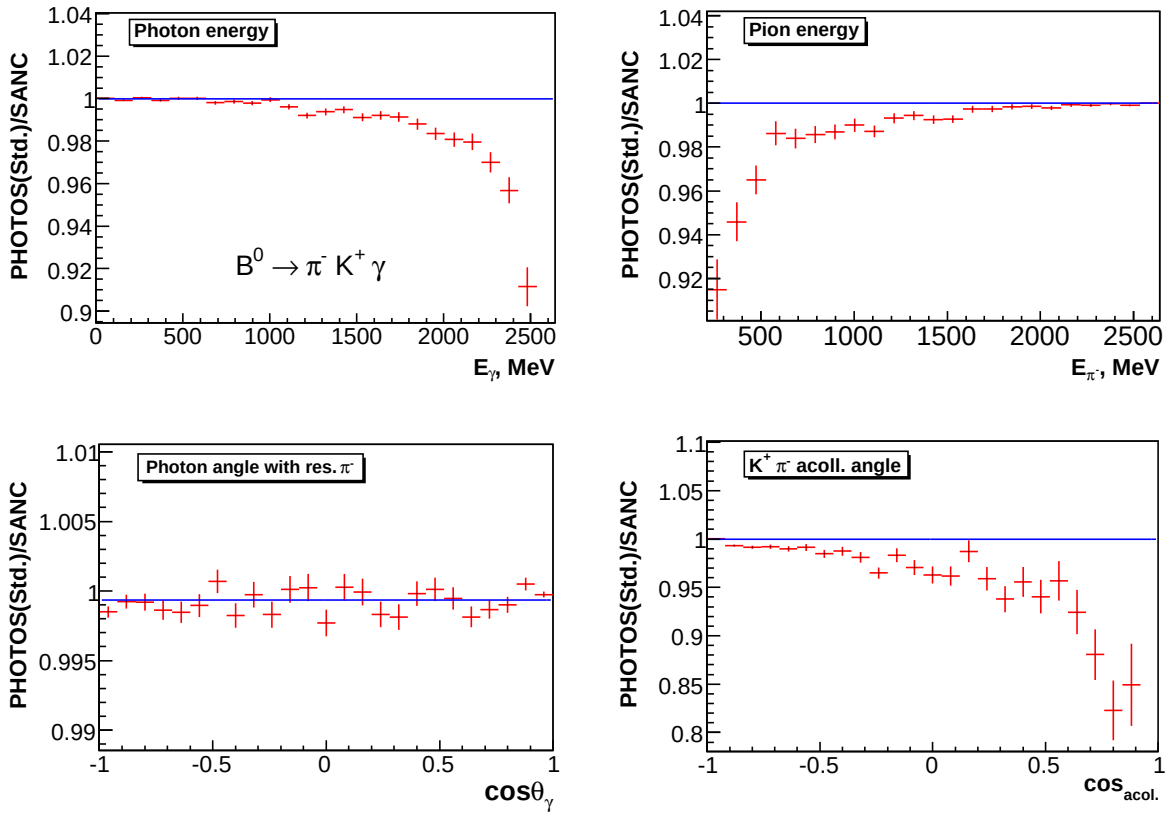

Figure 6: Results from PHOTOS with the exact matrix element, and SANC for ratios of the $B^0 \to \pi^- K^+(\gamma)$ distributions. Differences between PHOTOS and SANC are below statistical error for samples of 10^9 events.

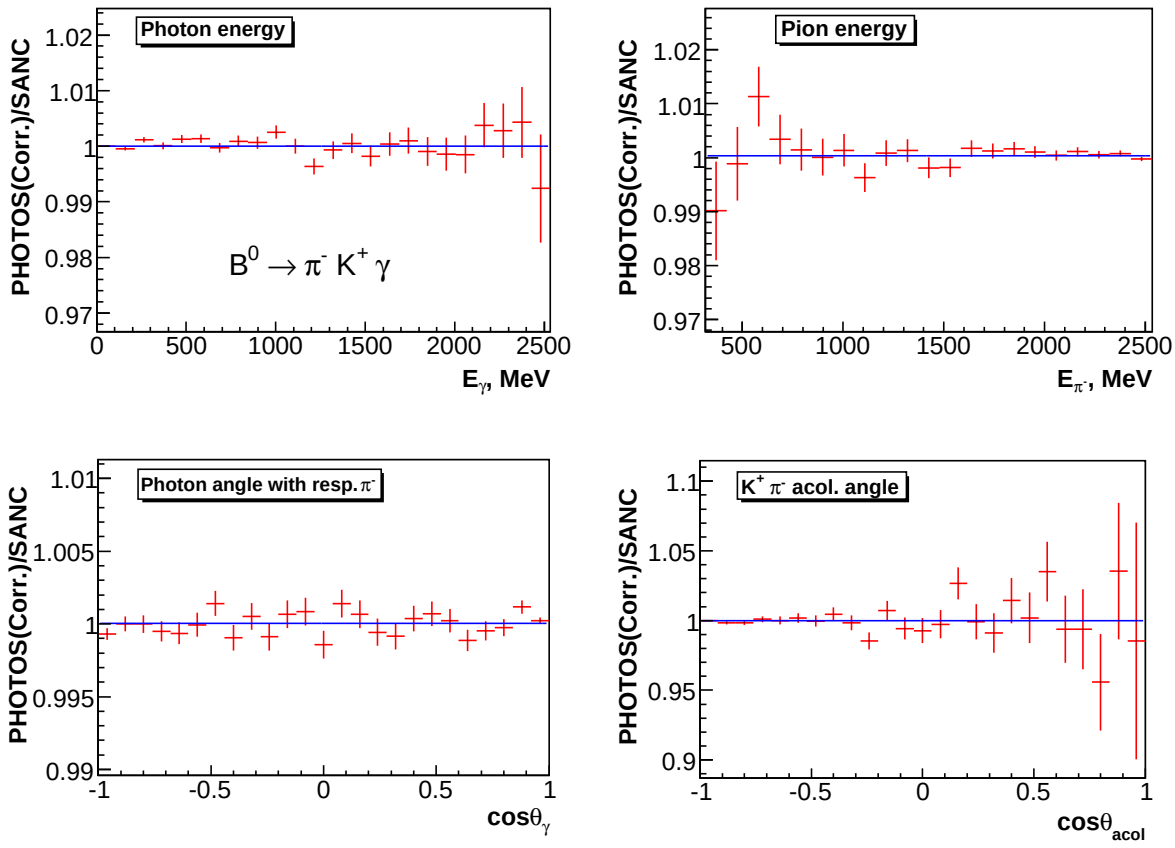

that level of technical sophistication. To establish it required a major effort. Kinematical variables used in PHOTOS differ from those of SANC. The differences could arise due to technical problems, also if for example the Born-level events which are to be modified by PHOTOS would not fulfill energy-momentum conservation or particles momenta were not on mass-shell, at the double precision level. This point must always be checked for every new installation of PHOTOS in an experimental environment. For that purpose we have collected numerical results, given in Table 1, for the cumulant of bremsstrahlung decay width: $G(E_{test}) = \Gamma(E_{test})/\Gamma^{\rm Total}$, where $\Gamma(E_{test})$ denotes the decay width, integrated over energy carried by all bremstrahlung photons combined up to maximum of E_{test}.

Channel	μ_{UV} [MeV]	E_{test} [MeV]	SANC	PHOTOS: $\mathcal{O}(\alpha)$	$\mathcal{O}(\alpha^2)$	$\mathcal{O}(exp)$
$B^- \to \pi^-\pi^0$	2500	2.6	0.9291	0.9289	0.9314	0.9311
$B^- \to \pi^-\pi^0$	2500	26	0.9571	0.9569	0.9578	0.9577
$B^- \to \pi^-K^0$	2500	2.6	0.9294	0.9292	0.9318	0.9314
$B^- \to \pi^-K^0$	2500	26	0.9574	0.9572	0.9580	0.9580
$B^- \to K^-\pi^0$	2500	2.6	0.9627	0.9628	0.9636	0.9634
$B^- \to K^-\pi^0$	2500	26	0.9777	0.9777	0.9779	0.9779
$B^- \to K^-K^0$	2500	2.6	0.9629	0.9631	0.9639	0.9638
$B^- \to K^-K^0$	2500	26	0.9779	0.9779	0.9782	0.9781
$B^0 \to \pi^-\pi^+$	900	2.6	0.8311	0.8306	0.8451	0.8433
$B^0 \to \pi^-\pi^+$	900	26	0.8978	0.8972	0.9019	0.9016
$B^0 \to \pi^-K^+$	900	2.6	0.8662	0.8660	0.8754	0.8741
$B^0 \to \pi^-K^+$	900	26	0.9193	0.9188	0.9219	0.9219
$B^0 \to K^-\pi^+$	900	2.6	0.8661	0.8659	0.8753	0.8743
$B^0 \to K^-\pi^+$	900	26	0.9193	0.9191	0.9220	0.9219
$B^0 \to K^-K^+$	900	2.6	0.9011	0.9014	0.9066	0.9057
$B^0 \to K^-K^+$	900	26	0.9407	0.9407	0.9424	0.9422

Table 1: *Benchmark results for B decays into pair of scalars: electromagnetic cumulative of decay width $\Gamma(E_{test})/\Gamma^{\rm Total}$, where E_{test} denotes the maximal energy which can be carried out by photons. The following input parameters were used: $m_B = 5279$ MeV, $m_{\pi^0} = 135$ MeV, $m_{\pi^\pm} = 139$ MeV, $m_{K^0} = 494$ MeV, $m_{K^\pm} = 498$ MeV. Our results differ negligibly between standard PHOTOS and the one with exact matrix element. That is why only one set of numerical results is provided. For each decay channel PHOTOS results of first, second and multiple photon radiation are to good precision proportional like $1-x : 1-x+x^2/2 : exp(-x)$, where x depends on the decay channel and E_{test}. To produce results for our table samples of 10^7 events were used. Statistical errors are thus at the level of the last significant digit for all the table entries.*

5. Summary

This paper was devoted to the study of bremsstrahlung corrections in the decay of B mesons into pair of scalars of rather large masses. Predictions were presented in the form of PHOTOS Monte Carlo.

To quantify the size of the Next to Leading logarithm effects normally missing in PHOTOS we have installed into the program the complete scalar-QED first order expression for the B decay matrix element. After modification, the differences between PHOTOS and the matrix element calculation embodied in SANC were below statistical error of 10^9 events for all of our benchmark distributions. Both PHOTOS and SANC were run at fixed first order without exponentiation. The agreement provides a technical test of the simulations from both of the two programs as well.

The improvement of the agreement due to the introduction of a correcting weight could come with a price. That was the case with the decay of Z. Because B mesons are scalar the complications did not materialize and a correcting weight can be installed to standard PHOTOS versions. On the other hand, numerically introduced improvements are small. Deficiencies of standard PHOTOS are localized in corners of bremsstrahlung phase space populated by photons of very high energies and angularly well separated from final state mesons. Those regions of the phase space weigh less than 0.005 to the total rate and differences in that region approach 20 % of their size, at most. The effects are thus significantly lower than 0.1 %, if quantified in units of the total B decay rate to a particular channel. Also, in those regions, the predictive power of scalar QED is rather doubtful. That is why we do not think it is urgent for users to change the PHOTOS correcting weight to enable the complete NLO, unless measured form-factors become available. Conribution to the systematic error of PHOTOS due to incompletness of the old kernel (with respect to scalar QED) does not depend on experimental cuts and is thus of no phenomenological importance for today.

Our paper was not only focused on numerical results due to final state bremsstrahlung in B decays. Aspects of mathematical organization of the program for calculation of radiative corrections for B production and decay was discussed as well. Approximations used in PHOTOS affects matrix elements and *not* phase space, which is treated exactly including all mass effects. Generation of the phase space starts from the tangent space constructed from an eikonal approximation but used for hard photons, even of energies above the available maximum enforced by energy momentum conservation. In the second step, phase-space constraints are enforced and compactification is introduced. This is similar to classical exclusive exponentiation. However, energy momentum constraints are introduced for each consecutive photon, step by step, and conformal symmetry is not exploited in that procedure.

Complete re-analysis of the final weight for decays into scalars was presented. Parts corresponding to matrix elements, phase space Jacobians and generator pre-samples were explicitly separated. Special care was devoted to mass terms. Analytic form of the single photon emission kernel (i. e. matrix element with approximation) used in standard version of PHOTOS, was also explicitly given. That is why, the analysis presented here can be easily extended to other decay channels. It is the first time that we have presented such a study for particles other

than elementary fermions and in the case where mass terms of order $\frac{\alpha}{\pi}\frac{m_{1,2}^2}{M_B^2}$ are not neglected.

For B decays in the case of multiple photon radiation in PHOTOS, a similar level of agreement as in Ref [14] for Z decay is expected, but the appropriate reference distributions do not exist yet. We agree with the results of reference [18], however only at the level of about 1 %. We have not performed any tuning of μ_{UV} and other input parameters used in that paper. Instead we have collected numerical results, given in Table 1, which can be used as a technical test of PHOTOS installation in particular simulation set-ups. We strongly recommend such tests to be performed. In these tests the agreement betweens PHOTOS and SANC (or simple semi-analytical expressions for higher order simulations) was significantly better than 0.1 % for all entries.

On the technical level it is worth mentioning that the NLO correcting weight of PHOTOS is used as an internal weight. All generated events remain weight 1, exactly as it was in the case of $Z \to \mu^+\mu^-$ decay. PHOTOS used for decays of B mesons into scalars provides an example of multiple emissions from both outgoing charged lines covering the complete phase space where the hard photon emisson region does not require any special treatment. Mass terms have been included without any approximations.

In principle, if necessary, complete higher order matrix elements (NNLO level) could be incorporated with the help of correcting weights as well. This interesting point definitely goes beyond the scope of the present paper and also beyond the phenomenological interest for any foreseeable future. This is equally true for the possible extensions to simulations in QCD, which are also outside the scope of the paper.

Acknowledgements.
Useful discussions with E. Barberio and F. Tkachov are acknowledged.

References

[1] E. Barberio, B. van Eijk, and Z. Was, *Comput. Phys. Commun.* **66** (1991) 115.

[2] E. Barberio and Z. Was, *Comput. Phys. Commun.* **79** (1994) 291–308.

[3] M. A. Dobbs *et al.*, hep-ph/0403045.

[4] CDF Collaboration, V. M. Abazov *et al.*, *Phys. Rev.* **D70** (2004) 092008, hep-ex/0311039.

[5] OPAL Collaboration, G. Abbiendi *et al.*, *Phys. Lett.* **B580** (2004) 17–36, hep-ex/0309013.

[6] DELPHI Collaboration, J. Abdallah *et al.*, *Eur. Phys. J.* **C31** (2003) 139–147, hep-ex/0311004.

[7] NA48 Collaboration, A. Lai *et al.*, *Phys. Lett.* **B602** (2004) 41–51, hep-ex/0410059.

[8] KTeV Collaboration, T. Alexopoulos *et al.*, *Phys. Rev.* **D71** (2005) 012001, hep-ex/0410070.

[9] Belle Collaboration, A. Limosani *et al.*, hep-ex/0504046.

[10] BABAR Collaboration, B. Aubert *et al.*, *Phys. Rev.* **D69** (2004) 111103, hep-ex/0403031.

[11] FOCUS Collaboration, J. M. Link *et al.*, hep-ex/0412034.

[12] P. Golonka and Z. Was, hep-ph/0508015.

[13] P. Golonka and Z. Was, *Eur. Phys. J.* **C45** (2006) 97–107, hep-ph/0506026.

[14] P. Golonka and Z. Was, hep-ph/0604232.

[15] A. Andonov *et al.*, *Comput. Phys. Commun.* **174** (2006) 481–517, hep-ph/0411186.

[16] T. Kinoshita, *J. Math. Phys.* **3** (1962) 650.

[17] T. D. Lee and M. Nauenberg, *Phys. Rev.* **B133** (1964) 1549.

[18] E. Baracchini and G. Isidori, *Phys. Lett.* **B633** (2006) 309–313, hep-ph/0508071.

[19] Z. Was, Written on the basis of lectures given at the 1993 European School of High Energy Physics, Zakopane, Poland, 12-25 Sep 1993, CERN-TH-7154-94.

[20] S. Jadach, Z. Was, R. Decker, and J. H. Kuhn, *Comput. Phys. Commun.* **76** (1993) 361–380.

[21] F. James, FOWL - a General Monte-Carlo Phase Space Program, 1977, CERN Computer Centre Program Library, Long Writeup W505.

[22] A. Andonov, S. Jadach, G. Nanava, and Z. Was, *Acta Phys. Polon.* **B34** (2003) 2665–2672, hep-ph/0212209.

[23] G. Nanava and Z. Was, *Acta Phys. Polon.* **B34** (2003) 4561–4570, hep-ph/0303260.